Contents lists available at ScienceDirect

Optics Communications

Invited Paper

3.5-GHz intra-burst repetition rate ultrafast Yb-doped fiber laser

Can Kerse [a,*], Hamit Kalaycıoğlu [b], Parviz Elahi [b], Önder Akçaalan [a], F. Ömer Ilday [a,b,*]

[a] Department of Electrical and Electronics Engineering, Bilkent University, Ankara 06800, Turkey
[b] Department of Physics, Bilkent University, Ankara 06800, Turkey

ARTICLE INFO

ABSTRACT

We report on an all-fiber Yb laser amplifier system with an intra-burst repetition rate of 3.5 GHz. The system is able to produce minimum of 15-ns long bursts containing approximately 50 pulses with a total energy of 215 μJ at a burst repetition rate of 1 kHz. The individual pulses are compressed down to the subpicosecond level. The seed signal from a 108 MHz fiber oscillator is converted to approximately 3.5 GHz by a multiplier consisting of six cascaded 50/50 couplers, and then amplified in ten stages. The highly cascaded amplification suppresses amplified spontaneous emission at low repetition rates. Non-linear interactions between overlapping pulses within a burst is also discussed.

1. Introduction

Fiber amplification of ultra-short pulses is becoming a mature technology in terms of practicality, cost effectiveness, offering high gain amplification, high powers and generally excellent beam quality [1–4]. Possibly, its most important application outside of the laser research laboratory, is material [5] and tissue [6] processing. Here, two drawbacks remain, *i.e.*, limited ablation rates and requirement for tens to hundreds of microjoules, which is still challenging for fiber technology and renders laser design complicated.

In their seminal 1999 paper [7], Marjoribanks and co-workers have demonstrated a powerful approach to material processing: The laser produces a group of high-repetition rate pulses, called a burst, which itself is repeated at a much lower repetition rate. This way, reasonable average powers are obtained despite the high repetition rates achieved during the burst. For a long time, burst-mode operation has been applied to diverse, but niche applications [8–14]. This is partly because, until recently, burst-mode laser systems have relied on complex solid state lasers, with architectures that were not optimized for burst mode. We developed the first burst mode fiber laser system [15], advanced it with electronic processing to achieve highly uniform intra-burst distribution [16], and scaled it to 1 MHz and 100 W for high power applications [17]. In the meantime, Limpert et al. demonstrated a

high-energy rod-fiber type burst-mode amplifier [18]. Recently, we reported a detailed investigation on the limits of pulse-pumped [19] and continuously pumped [20] all-fiber burst mode laser system. By focusing on the pulse-material interaction physics, we have identified a new regime of laser–material interaction, which we refer to as ablation-cooled laser material removal [21,22]. In this regime, the repetition rate has to be high enough that there is insufficient time for the targeted spot size cool down substantially by heat conduction into the rest (bulk) of the target material by the time the next pulse arrives. As a result, the individual pulse energy ablation threshold is scaled down by several orders of magnitude if the repetition rate is simultaneously increased, while thermal effects to the bulk of the target are also reduced. Furthermore, the simultaneous reduction of pulse energy and the pulse-to-pulse spacing reduces plasma shielding effects.

Ultrafast burst-mode lasers shown to date are limited to the order of 100 MHz or even lower intra-burst repetition rates. Considering that metals and many other technologically important materials, particularly, silicon have high thermal diffusivity, thermal relaxation times can be in the nanosecond range, which requires the repetition rates to be in the few-GHz range to fully exploit the ablation cooling effect. In order to obtain such high intra-burst rates with ultrafast pulses, one needs mode-locked seed signals at the desired repetition rate. SESAM-mode-locked semiconductor disk lasers and vertical-external-cavity surface-emitting lasers have achieved few picosecond and sub-picosecond pulse durations at multi-GHz repetition rates [23], but they are specialized solutions and an all-fiber architecture is highly desirable. Femtosecond fiber lasers with around 1 GHz repetition rate have been developed [24], but further scaling seems extremely

difficult. Thus, direct generation of femtosecond pulses at multi-GHz repetition rates faces practical challenges. It is possible to use Fabry–Perot and other passive cavities to scale up the repetition rate with excellent fidelity and low noise, but this approach is quite complex [25,26]. The only simple and all-fiber-based method appears to be the use of pulse repetition rate multiplication (PRRM) via cascaded couplers [27–29]. Among such methods, multiplication with cascaded 3-dB fiberoptic couplers offers a simple and effective solution by an integer multiplication factor of $2^{(N-1)}$, where N is the number of couplers [27,28].

In this contribution, we demonstrate an all-fiber Yb burst mode laser amplifier system with an intra-burst repetition rate of 3.5 GHz, which is optimized for low amplified spontaneous emission (ASE) operation at low burst repetition rates. The system is able to produce a minimum of 15-ns long bursts with a total energy of 215 μJ at a burst repetition rate of 1 kHz. The individual pulses are compressible down to sub-picosecond level. The seed signal from a 108-MHz fiber oscillator is converted to 3.5 GHz by a fiber-optic multiplier consisting of six cascaded 3 dB couplers, and then amplified in ten stages. The amplifier system has a highly cascaded fiber-integrated architecture designed to achieve high-energy bursts made of high energy pulses, while suppressing ASE. Pulsed pumping that is synchronized with the seed by an FPGA-based electronic system is employed in the six subsequent amplifier stages. Pump pulses are optimized to obtain the highest signal-to-ASE ratio, while ASE is monitored closely at the output of the system. The disadvantage of the repetition rate multiplier approach adopted here is the difficulty to maintain equal pulse

energies and equal temporal separations due to coupling efficiency asymmetries between the arms of the couplers and the difficulty to get precise fiber lengths between the couplers. These effects lead to variations in the pulse energies within a burst and in the temporal spacing between the pulses. While these deviations are quite small, given the presence of non-linear effects in the amplifier, it was not clear a priori whether these could lead to amplified variations or even instabilities. As discussed below, it is shown that this is not the case, at least, up to moderate non-linearities (of $\sim\pi$ non-linear phase shift).

2. Experimental setup

The experimental setup is summarized in Fig. 1(a) and consists of an all-normal dispersion laser oscillator [30], which generates a mode-locked signal at a repetition rate of 108 MHz as the seed source. The signal from the oscillator is converted to 3.5 GHz by a six-stage cascaded repetition rate multiplier and a devoted pre-amplifier at the end of the couplers to compensate for losses of the multiplier. This source seeds nine amplifier stages, comprising of six core-pumped pre-amplifiers and three double-clad (DC) fiber power amplifiers along with synchronized pulse picking and pulsed-pumping electronics. The all-fiber master-oscillator power-amplifier Yb-fiber architecture is based on the original design in [31]. The first three stages of pre-amplifiers utilize continuous pumping while the latter three, which are positioned after the acousto-optic modulator (AOM), incorporate pulsed pumping. The
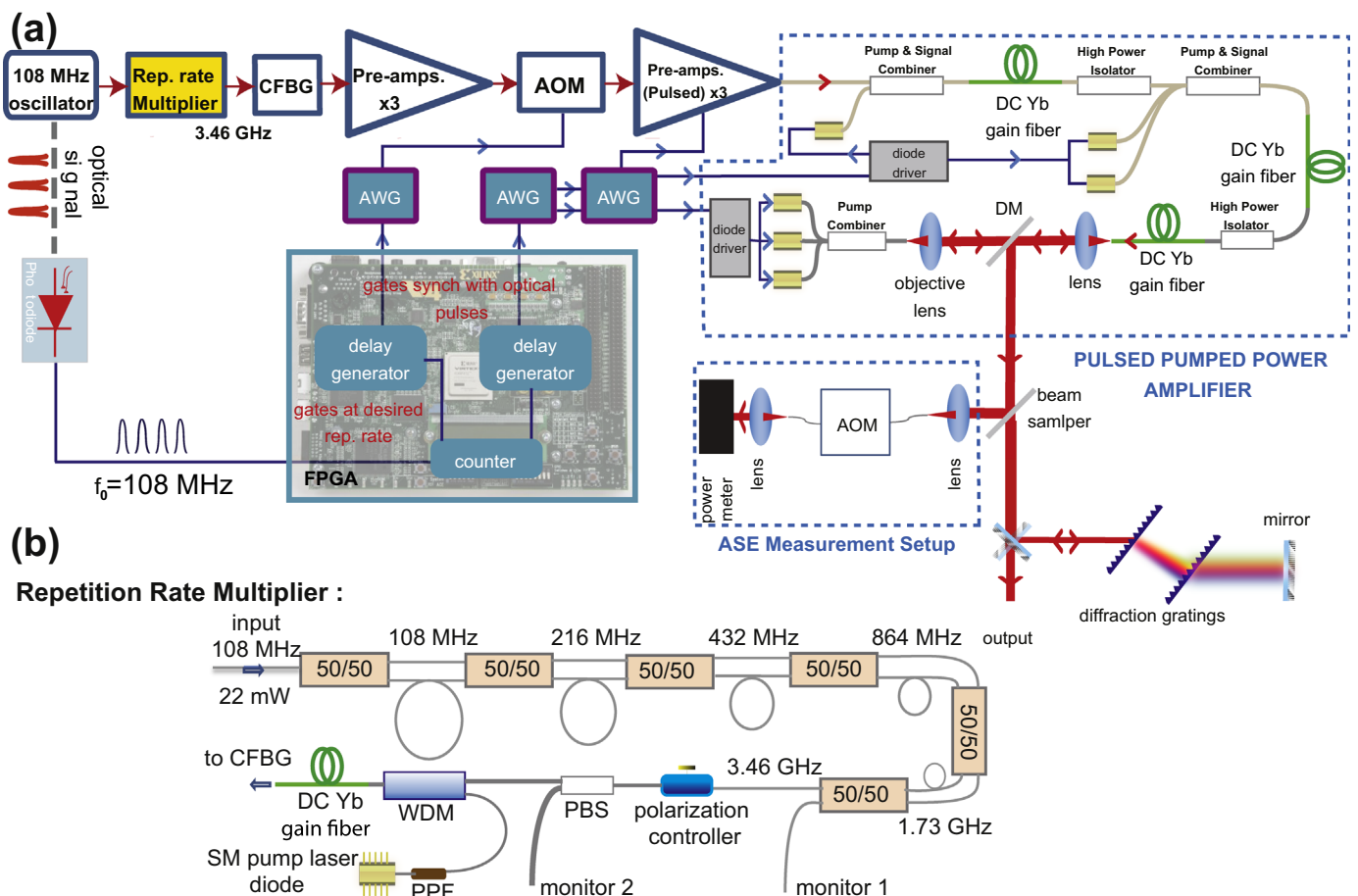

Fig. 1. (a) Schematic diagram of the experimental setup. CFBG: chirped fiber Bragg grating, AOM: acousto-optical modulator, AWG: arbitrary waveform generator, FPGA: field programmable gate array, DM: dichroic mirror, WDM: wavelength division multiplexer, PBS: polarizing beam splitter, PPF: pump protection filter, SM: single-mode, DC: double-clad. (b) Schematic setup of high repetition rate multiplier followed by first stage fiber amplifier.

mode-locked fiber oscillator generates 22 mW, 3.6 ps-long chirped pulses. The spectral bandwidth is 20 nm, which is centered at 1030 nm. Output from the oscillator leads to the repetition rate multiplier (Fig. 1(b)) consisting of cascaded 3-dB couplers, where for each coupler there is a length difference between the two output arms, equivalent to a delay of half of period of the signal repetition rate at the input of that coupler. Therefore, the repetition rate is doubled at each stage, beginning with the second coupler and in this case, with six cascaded couplers, it is multiplied by 2^5, increasing from 108 MHz to 3.5 GHz. Finally, 7.5 mW of output power from the repetition rate multiplier is polarized with an in-line polarization beam splitter (PBS), following a polarization controller. It is then amplified to 300 mW in the first amplifier stage, which comprises 30-cm long core-pumped Yb-doped fiber (Yb-401PM, CorActive, Inc., peak absorption of 570 dB/m at 976 nm) before entering the pulse stretcher. After the PBS, the system consists solely of polarization maintaining (PM) components.

The output pulses from the first amplifier are stretched to about 2 ns in a chirped fiber Bragg grating (CFBG) designed to match the dispersion of a compressor consisting of a pair 1800 l/mm transmission gratings with a separation of 70 cm at an incidence angle of 69°. The seed signal drops below 50 mW and the spectrum is ~15 nm wide at the output of the pulse stretching unit made of a circulator and the CFBG. Thereafter, it is amplified by three stages of preamplifiers (all comprising of core-pumped Yb-401PM) to above 1 W before entering the AOM. The pulse picking and pulse pumping processes are both synchronized with the 108-MHz oscillator using a field programmable gate array (FPGA) circuit, which delivers the trigger signals to arbitrary waveform generators (AWG). The AWGs, in turn, drive the AOM and diode drivers. This electronic configuration enables us to adjust burst duration and the burst repetition frequency freely. The AOM, which imprints the desired pulse burst envelope onto the signal has rise and fall times of 6 and 8 ns, respectively. With the AOM imposing bursts repeated at 1 kHz, the duty cycle of the signal drops sharply to 0.01% level, hence, the bursts are amplified in six stages of pulsed amplification. Comparatively short gain fibers are

used in the three-stage pulsed preamplifier following the AOM to suppress ASE generation. The power amplifier at the end of the system consists of three stages also, first two forward-pumped and final one backward-pumped, which employ one, two and three 25-W pump diodes, respectively. The three stages use Yb-1200-DC-20/125PM (NLight, Inc., peak absorption of 11.1 dB/m at 976 nm) as gain fiber with lengths shorter than that required for high efficiency in continuous pumping regime. To monitor ASE, 1% of the output power is diverted to the another AOM, while the signal is delayed with respect to the diode drivers by an adjustable amount. A pair of transmittance gratings with 1800 line/mm is employed to dechirp and compress the output pulses. Further details on the amplifier system, the electronic control and synchronization unit can be found in our earlier work [19].

3. Results

In order to characterize the repetition rate multiplier, the pulse train is measured after the multiplier using a 50-GHz bandwidth digital serial analyzer (Tektronix, Inc., DSA8200) along with an InGaAs photodetector (Electro-Optics Technology, Inc., ET-3500F) for a train of 32 (2^5) pulses, which constitute one full cycle of the repeated pulse train of the oscillator (Fig. 2(a)). The average values and standard deviation are calculated to be 0.92 and 0.03 for normalized intensity, and 285.3 ps and 9.4 ps for the temporal separation between the pulses (which define the average repetition rate), respectively (Fig. 2(b)). In other words, both pulse energy and temporal spacing deviate no more than ~3% as a result of the imperfections in the repetition rate multiplication, which is a very acceptable result for typical amplification of a burst-mode laser. Fig. 2(c) shows a 20-GHz span of the RF spectrum recorded with 100 kHz resolution bandwidth. A close-up RF spectrum of the fundamental frequency with 20 Hz resolution and 10 kHz span is presented in Fig. 2(d).

After characterization and optimization of all the signal durations and frequencies, the system is able to amplify 15 ns-long bursts comprising of 50 pulses to a net energy of 215 μJ at a burst
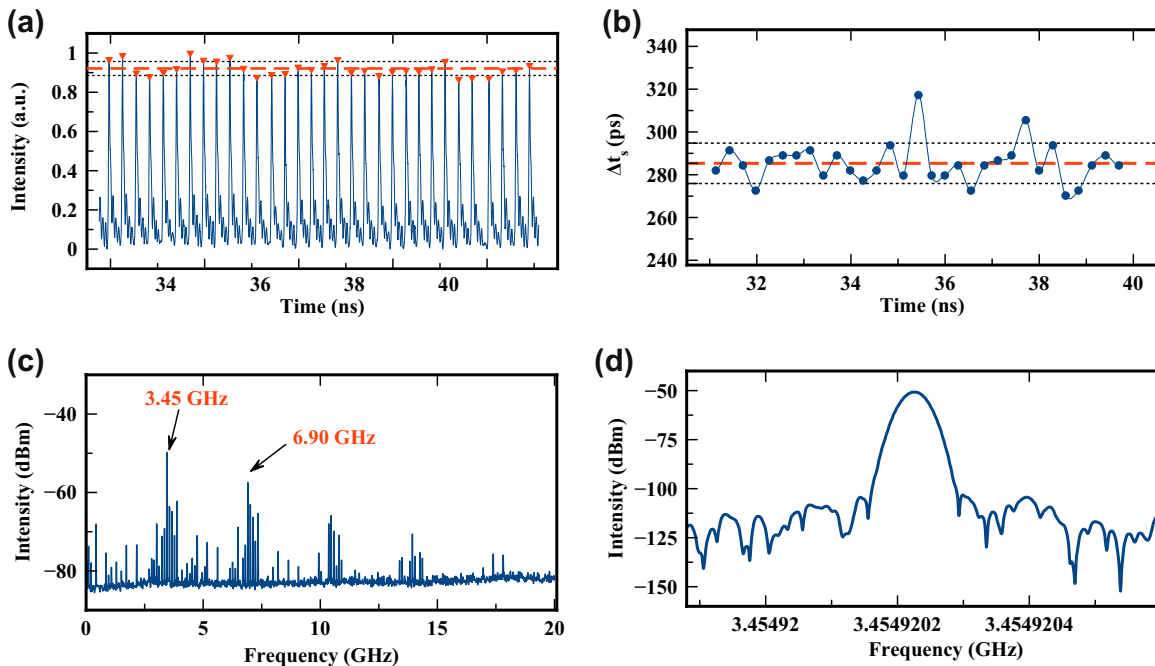

Fig. 2. (a) Temporal profile of 3.5-GHz pulse train measured after the repetition rate multiplier. (b) Measured deviation from average pulse separation time. Dashed (red) line indicates average and dotted (black) line indicates one standard deviation. (c) Measured RF spectrum with 20 GHz span and 100 kHz resolution. (d) Measured close-up RF spectrum with 10 kHz span and 20 Hz resolution. (For interpretation of the references to color in this figure caption, the reader is referred to the web version of this paper.)
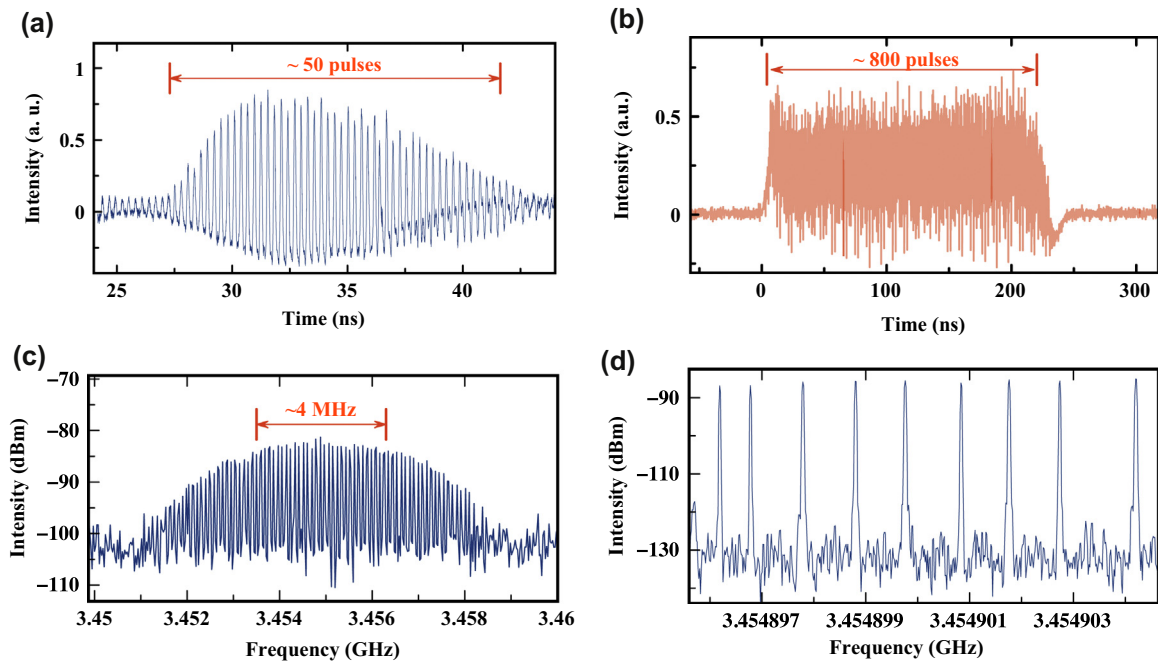
Fig. 3. (a) Measured output pulse train for the 15 ns-long burst after dechirping. (b) 230 ns-long burst train containing approximately 800 pulses. (c) Measured RF spectra of the amplified burst train over a span of 10 MHz, centered at 3.455 GHz, the width of which is determined by the burst duration of 230 ns. (d) Close-up of the RF spectrum in (c) showing densely spaced comb lines of 1-kHz spacing over a span of 10 kHz.

repetition rate of 1 kHz. This is the shortest possible burst duration allowed by the response time of the AOM. For this reason, burst pre-shaping [16] was not possible. Hence, an electronic gate in the form of a 15-ns wide rectangular pulse was applied to the AOM, which results in the burst shape seen in Fig. 3(a) with a Gaussian-like pulse distribution and nearly 15 ns duration. The maximum and average pulse energy inside the burst is calculated to be 8.4 μJ and 4.4 μJ, respectively. The laser system is also able to produce arbitrarily long bursts, containing an increasing number of pulses. Temporal profile of a 230 ns-long burst, containing 800 pulses for a total, ASE-free energy of 490 μJ is shown in Fig. 3(b). As a result of the much longer burst duration, it is possible to apply pre-shaping in this case, which results in much more uniform energy distribution compared to the 15-ns long burst. The maximum and the average pulse energy inside the 230-ns long burst is calculated as 1.1 μJ and 0.56 μJ, respectively. While we focus on the 3.5-GHz intra-burst repetition rate, we note that the present system is flexible in this regard. Much higher per pulse energies can be extracted by using a lower repetition rate multiplication. For example, pulse energies above 10 μJ can readily be obtained with an intra-burst repetition rate of 1.7 GHz, and up to 16 μJ pulses can be compressed below the pico-second level (at an intra-burst repetition rate of 0.8 GHz).

We provide further characterization of the bursts in the RF domain. Recorded RF spectra of the amplified burst train over a span of 10 MHz, centered at 3.455 GHz, displays the comb generated by the burst system (Fig. 3(c)). The frequency domain representation of a train of 230 ns-long pulse bursts repeated at 1 kHz is shown under an envelope with a 3-dB bandwidth of ~4 MHz, as determined by the temporal shape of the burst envelope. Fig. 3(d) presents the close-up RF spectrum of the output burst with 1 kHz lines with a span of 10 kHz. Note that the comb lines are actually much denser than as displayed in the figure, which is due to the finite number of sample points that the spectrum analyzer (FSUP26, Rohde & Schwarz, Inc) is able to capture. The measured autocorrelation for 200 μJ burst energy, 15-ns long, 50-pulses is shown in Fig. 4(a). The full-width at half-maximum (FWHM) pulse duration is estimated to be 450 fs, assuming a Gaussian pulse shape. The measured, corresponding optical spectrum is shown in Fig. 4(b).

Finally, we note that the stretched pulse duration (2 ns) exceeds the pulse repetition period (285 ps) substantially, causing overlap between stretched neighboring pulses (approximately 7 of them). This situation can easily be avoided through the use of another CFBG with lower dispersion. However, the present situation raises interesting questions on the extent and nature of interaction between pulses
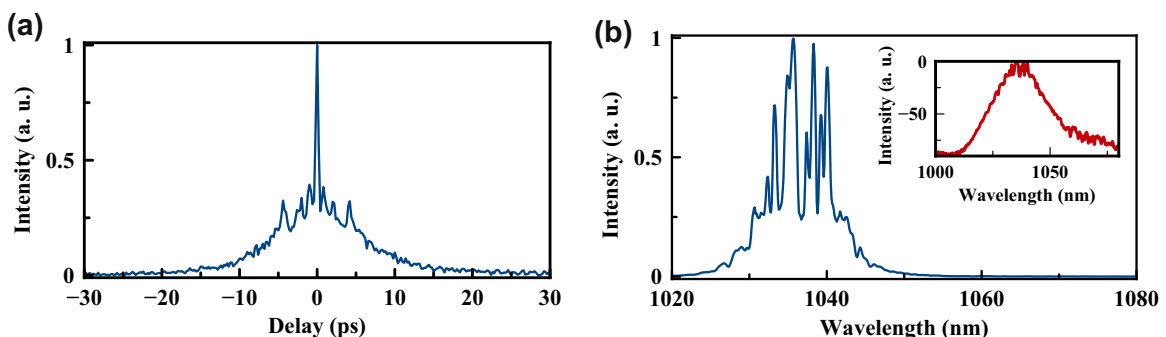

Fig. 4. (a) Measured autocorrelation for a burst energy of 200 μJ, burst duration of 15-ns, and containing approximately 50 pulses per burst. (b) Measured output optical spectrum for the same conditions as in (a). Inset: semi-log version.
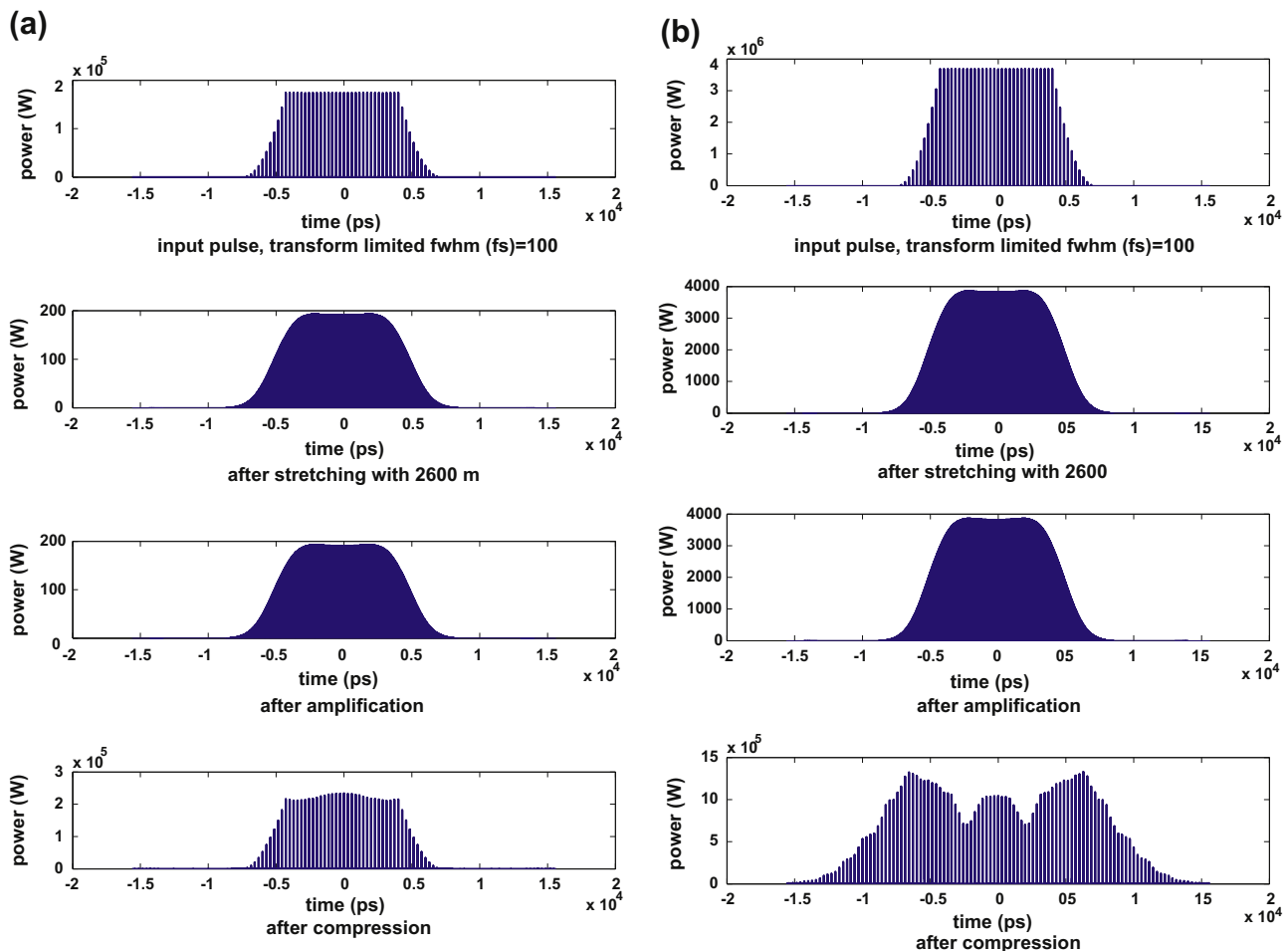
(a)

(b)

Fig. 5. Simulation results for 50-pulse bursts with intra-burst pulse repetition period of 285 ps, with the pulses being stretched to 2 ns, then traversing a nonlinear optical segment, before being dechirped, for (a) low nonlinear phase shift in the amplifier, and (b) 20 times higher nonlinear phase shift in the amplifier.

throughout the amplification process and whether the pulses can be captured back and narrow pulses similar to the non-overlapping cases can be obtained after compression. Experimentally, this is indeed the case, as discussed above. The complex temporal structure that shows up as pedestal formation points towards non-linear interaction between neighboring pulses within the burst. One should also keep in mind that the autocorrelation reflects an average of the pulses within the burst, which have a considerable energy variation as shown in Fig. 2(b). The corresponding spectrum for the 200 µJ bursts in Fig. 4 (b) also exhibits a highly structured form in parallel, and a filtered-down bandwidth due to the multistage amplification as well. As a first attempt to get further insight on the pulse interaction, we have used numerical simulations of the non-linear Schrödinger equation for 50 pulsed-bursts. We consider, as simplification, that the stretcher only exhibits GVD, which is followed by a medium with only Kerr non-linearity and a compressor also with only GVD. The preliminary simulation results shown in Fig. 5 indicate the possibility of energy transfer between overlapping pulses when nonlinearity reaches approximately π. For the results presented here, the overall effect is small, but this phenomenon will be investigated in a dedicated contribution that focusses on the underlying physics.

4. Conclusion

In conclusion, we have demonstrated, to our knowledge, the first burst-mode fiber laser system achieving multi-GHz-level

repetition rates. The system produces bursts of pulses at 1 µm wavelength and is capable of generating as short as 15 ns-long bursts with intra-burst pulse repetition rate of 3.5 GHz with 215 µJ energy at 1 kHz repetition rate. This combination of parameters constitute a unique capability, which has been specifically developed to exploit ablation-cooled laser material removal [21,22]. We expect the laser architecture demonstrated here to find applications in ultrafast laser-material and laser-tissue processing.

References

[1] D.J. Richardson, J. Nilsson, W.A. Clarkson, High power fiber lasers: current status and future perspectives (invited), J. Opt. Soc. Am. B 27 (2) (2010) B63–B92.
[2] J. Nilsson, D.N. Payne, High-power fiber lasers, Science 332 (6032) (2011) 921–922.
[3] M.E. Fermann, I. Hartl, Ultrafast fibre lasers, Nature Photon. 7 (11) (2013) 868–874.
[4] C. Jauregui, J. Limpert, A. Tuennermann, High-power fibre lasers, Nature Photon. 7 (11) (2013) 861–867.

[5] K. Sugioka, Y. Cheng, Ultrafast Laser Processing, CRC Press, Boca Raton, FL, 2013 33487-2742.

[6] S.H. Chung, E. Mazur, Surgical applications of femtosecond lasers, J. Biophotonics. 2 (10) (2009) 557–572.

[7] M. Lapczyna, K.P. Chen, P.R. Herman, H.W. Tan, R.S. Majoribanks, Ultra high repetition rate (133 MHz) laser ablation of aluminum with 1.2-ps pulses, Appl. Phys. A 69 (1999) S883–S886.

[8] H. Braun, L. Rinolfi, S. Weisz, A. Ferrari, R. Tomas, CLIC 2008 parameters, CERN OPEN 021, 2008.

[9] I. Will, H.I. Templin, S. Schreiber, W. Sandner, Photoinjector drive laser of the FLASH FEL, Opt. Express. 19 (24) (2011) 23770–23781.

[10] P. Wu, W.L. Lempert, R.B. Miles, Megahertz pulse-burst laser and visualization of shock-wave boundary-layer interaction, AIAA J. 38 (4) (2000) 672–679.

[11] B.S. Thurow, A. Satija, K. Lynch, Third-generation megahertz-rate pulse burst laser system, Appl. Opt. 48 (11) (2009) 2086–2093.

[12] D.J. Den Hartog, J.R. Ambuel, M.T. Borchardt, A.F. Falkowski, W.S. Harris, D.J. Holly, E. Parke, J.A. Reusch, P.E. Robl, H.D. Stephens, Y.M. Yang, Pulse-burst laser systems for fast Thomson scattering (invited), Rev. Sci. Instrum. 81 (10) (2010) 10D513.

[13] M. Murakami, B. Liu, Z. Hu, Z. Liu, Y. Uehara, Y. Che, Burst-mode femtosecond pulsed laser deposition for control of thin film morphology and material ablation, Appl. Phys. Express. 2 (4) (2009) 042501.

[14] T. Liu, J. Wang, G.I. Petrov, V.V. Yakovlev, H.F. Zhang, Photoacoustic generation by multiple picosecond pulse excitation, Med. Phys. 37 (4) (2010) 1518–1521.

[15] H. Kalaycioglu, K. Eken, F.Ö. Ilday, Fiber amplification of pulse bursts up to 20 μJ pulse energy at 1 kHz repetition rate, Opt. Lett. 36 (17) (2011) 3383–3385.

[16] H. Kalaycioglu, Y.B. Eldeniz, Ö. Akcaalan, S. Yavas, K. Gurel, M. Efe, F.Ö. Ilday, 1 mJ pulse bursts from a Yb-doped fiber amplifier, Opt. Lett. 37 (13) (2012) 2586–2588.

[17] P. Elahi, S. Ylmaz, Y.B. Eldeniz, F.Ö. Ilday, Generation of picosecond pulses directly from a 100 W, burst-mode, doping-managed Yb-doped fiber amplifier, Opt. Lett. 39 (2) (2014) 236–239.

[18] S. Breitkopf, A. Klenke, T. Gottschall, H.-J. Otto, C. Jauregui, J. Limpert, A. Tuennermann, 58 mJ burst comprising ultrashort pulses with homogenous energy level from an Yb-doped fiber amplifier, Opt. Lett. 37 (24) (2012) 5169–5171.

[19] H. Kalaycıoğlu, Ö. Akcaalan, S. Yavas, Y.B. Eldeniz, F.Ö. Ilday, Burst-mode Yb-doped fiber amplifier system optimized for low-repetition-rate operation, J. Opt. Soc. Am. B 32 (5) (2015) 900–906.

[20] S. Yilmaz, P. Elahi, H. Kalaycıoğlu, F.Ö. Ilday, Amplified spontaneous emission in high-power burst-mode fiber lasers, J. Opt. Soc. Am. B 32 (12) (2015) 2462–2466.

[21] C. Kerse, H. Kalaycioglu, P. Elahi, Ö. Akcaalan, S. Yavas, M.D. Asik, D.K. Kesim, K. Yavuz, B. Cetin, F.Ö. Ilday, Ablation-cooled material removal at high speed with femtosecond pulse bursts, in: Advanced Solid State Lasers (Optical Society of America, 2015), paper AF2A.5.

[22] C. Kerse, H. Kalaycioglu, P. Elahi, S. Yavas, D.K. Kesim, Ö. Akcaalan, B. Öktem, M.D. Ask, H. Hoogland, R. Holzwarth, F.Ö. Ilday, Ablation-cooled material removal with ultrafast bursts of pulses, submitted for publication.

[23] M. Mangold, C.A. Zaugg, S.M. Link, M. Golling, B.W. Tilma, U. Keller, Pulse repetition rate scaling from 5 to 100 GHz with a high-power semiconductor disk laser, Opt. Express. 22 (2014) 6099–6107.

[24] C. Li, Y. Ma, X. Gao, F. Niu, T. Jiang, A. Wang, Z. Zhang, 1 GHz repetition rate femtosecond Yb: fiber laser for direct generation of carrier-envelope offset frequency, Appl. Opt. 54 (2015) 8350–8353.

[25] J. Chen, J.W. Sickler, P. Fendel, E.P. Ippen, F.X. Kartner, T. Wilken, R. Holzwarth, T.W. Hansch, Generation of low-timing-jitter femtosecond pulse trains with 2 GHz repetition rate via external repetittion rate multiplication, Opt. Lett. 33 (9) (2008) 959–961.

[26] J. Lee, S.-W. Kim, Y.-J. Kim, Repetition rate multiplication of femtosecond light pulses using a phase-locked all-pass fiber resonator, Opt. Express. 23 (2015) 10117–10125.

[27] S.-S. Min, Y. Zhao, S. Fleming, Repetition rate multiplication in figure-eight fibre laser with 3 dB couplers, Opt. Commun. 277 (2) (2007) 411–413.

[28] A. Haboucha, W. Zhang, T. Li, M. Lours, A.N. Luiten, Y. Le Coq, G. Santarelli, Optical-fiber pulse rate multiplier for ultralow phase-noise signal generation, Opt. Lett. 36 (18) (2011) 3654–3656.

[29] R. Maram, J. Van Howe, M. Li, J. Azaña, Lossless fractional repetition-rate multiplication of optical pulse trains, Opt. Lett. 40 (3) (2015) 375–378.

[30] A. Chong, J. Buckley, W. Renninger, F. Wise, All-normal-dispersion femtosecond fiber laser, Opt. Express. 14 (21) (2006) 10095–10100.

[31] F.Ö. Ilday, H. Lim, J.R. Buckley, F.W. Wise, Practical all-fiber source of high-power, 120-fs pulses at 1 μm, Opt. Lett. 28 (15) (2003) 1362–1364.